Materials Science and Engineering C xxx (2008) xxx–xxx

Contents lists available at ScienceDirect

Materials Science and Engineering C

journal homepage: www.elsevier.com/locate/msec

Physical characterization of hydroxyapatite porous scaffolds for tissue engineering

S. Teixeira [a,b,*], M.A. Rodriguez [c], P. Pena [c], A.H. De Aza [c], S. De Aza [c], M.P. Ferraz [a,d], F.J. Monteiro [a,b]

[a] INEB — Instituto de Engenharia Biomédica, Divisão de Biomateriais; Universidade do Porto, Rua do Campo Alegre, 823, 4150-180 Porto, Portugal
[b] Universidade do Porto, Faculdade de Engenharia, Departamento de Engenharia Metalúrgica e Materiais, Porto, Portugal
[c] Instituto de Cerámica y Vidrio, CSIC, 28049-Cantoblanco, Madrid, Spain
[d] Faculdade de Ciências da Saúde da Universidade Fernando Pessoa, Rua Carlos da Maia, 296, 4200-150 Porto, Portugal

ARTICLE INFO

Article history:
Received 29 January 2008
Received in revised form 1 July 2008
Accepted 30 September 2008
Available online xxxx

Keywords:
Hydroxyapatite
Porous scaffolds
Tissue engineering

ABSTRACT

The present study refers to the preparation and characterization of porous hydroxyapatite scaffolds to be used as matrices for bone regeneration or as specific release vehicles.
Ceramics are widely used for bone tissue engineering purposes and in this study, hydroxyapatite porous scaffolds were produced using the polymer replication method. Polyurethane sponges were used as templates and impregnated with a ceramic slurry at different ratios, and sintered at 1300 °C following a specific thermal cycle.
The characteristics of the hydroxyapatite porous scaffolds and respective powder used as starting material, were investigated by using scanning electron microscopy, particle size distribution, X-ray diffraction, Fourier transformed infrared spectroscopy and compressive mechanical testing techniques. It was possible to produce highly porous hydroxyapatite scaffolds presenting micro and macropores and pore interconnectivity.

1. Introduction

Bone tissue engineering is a promising area that aims at developing implants capable of repairing and/or substituting damaged or lost bone tissue.

Some current strategies include the use of autografts and allografts; however, these options contain some disadvantages, namely, tissue availability, diseases transmission and donor morbidity. As a result, there is the need to develop alternative strategies for the repair of damaged bone tissue, namely the use of scaffolds.

However, when developing porous matrices for the specific case of bone tissue engineering, some criteria must be met, namely porosity, allowing cells to migrate through the pores, good conditions for nutrient transport, tissue infiltration and ultimately, vascularization [1,2].

Several techniques have been developed in order to meet the required criteria and produce porous scaffolds, such as the use of gel casting [3,4], gas foaming [5], slip casting [6,7], fiber compacting [8], solid free form fabrication [4–9] and freeze casting [10].

On the other hand, the polymer replication method offers the possibility of producing a tailored scaffold with controllable pore size using a polyurethane sponge as a template [11–13].

Calcium phosphates are among the most widely used materials for bone tissue regeneration. They can be manufactured as gels, pastes, and solid blocks or even as porous matrices, with orthopaedics and dentistry being their main areas of application. Hydroxyapatite (HA) and other calcium derivatives (tricalcium phosphates, etc.) are the most commonly used calcium phosphates, due to their calcium/phosphorus (Ca/P) ratios that are close to that of natural bone and also their stability when in contact with physiological environment.

HA is a major constituent of bone materials and is resorbed after a long time of residence in the body, demonstrating its biocompatibility [14–17].

In this study, porous hydroxyapatite scaffolds were obtained using the polymer replication method and were characterized. These scaffolds may be used as matrices for bone tissue engineering or as specific release vehicles [11,12,18]. Also, they may be functionalized with molecules of interest such as collagen, chitosan, etc, in order to improve their biological response [19–24].

The characteristics of the hydroxyapatite porous scaffolds and hydroxyapatite powder that was used as starting material were assessed by means of scanning electron microscopy (SEM), particle size distribution, X-ray diffraction (XRD), Fourier transformed infrared spectroscopy (FTIR) and compressive mechanical testing techniques. It was possible to obtain, using porous polymer sponge as a template,

* Corresponding author. INEB — Instituto de Engenharia Biomédica, Divisão de Biomateriais; Universidade do Porto, Rua do Campo Alegre, 823, 4150-180 Porto, Portugal.
E-mail address: smsilva@ineb.up.pt (S. Teixeira).

0928-4931/$ – see front matter © 2008 Elsevier B.V. All rights reserved.
doi:10.1016/j.msec.2008.09.052

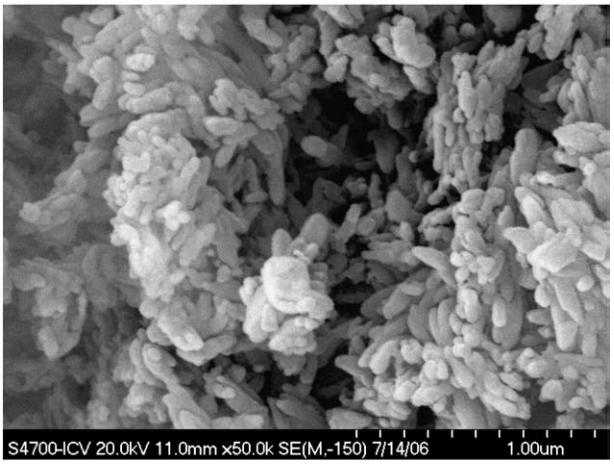

Fig. 1. Scanning electron microscopy image of the hydroxyapatite powders used in the ceramic slurry preparation. The powders organize themselves into aggregates.

highly porous hydroxyapatite scaffolds with micro and macroporosity in addition to interconnectivity.

2. Materials and methods

2.1. Sample preparation

The scaffolds were prepared using polyurethane sponges as a template. These polyurethane sponges (with an average pore size of 200 μm), kindly provided by Recticel (Belgium), were impregnated with ceramic slurry as previously reported [11–13,25].

The hydroxyapatite powders (P120, Plasma Biotal) were sieved until a particle size smaller than 75 μm was achieved. Afterwards, a ceramic slurry composed by hydroxyapatite (g), water (mL) and surfactant (mL, LM-3, Neodisher) was prepared. Several composition ratios were impregnated onto the polyurethane sponges and the 6 g (HA):4 mL (H_2O): 0.2 mL (tensioactive) ratio was considered as the best scaffold produced due to its adequate strength to withstand manipulation. The polyurethane sponge was squeezed to remove slurry excess and treated according to the following sintering cycle: heating at 1 °C/min followed by a 1 h plateau at 600 °C; heating at 4 °C/min followed by another plateau of 1 h at 1300 °C. Then, power was turned off and the samples were allowed to cool inside the furnace for 24 h. Next, the scaffolds were cut into 5 mm cubes with a sharp razor.

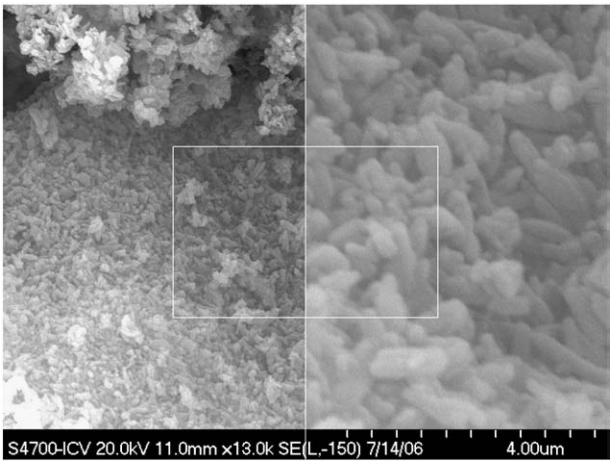

Fig. 2. Scanning electron microscopy image of the hydroxyapatite powders used in the ceramic slurry preparation. On the left side (13,000×) the hydroxyapatite aggregates may be visualised and on the right side (65,000×) a more detailed view of the hydroxyapatite aggregates is seen.

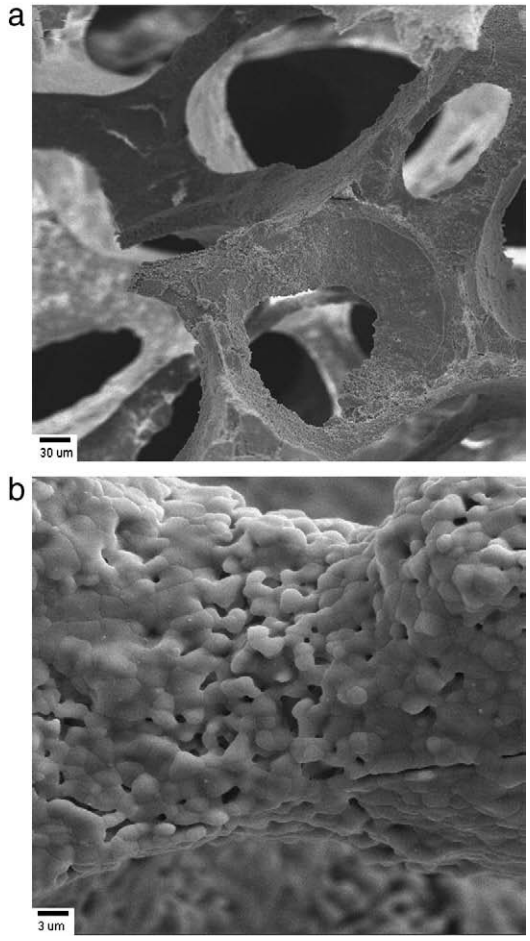

Fig. 3. Scanning electron microscopy of the hydroxyapatite scaffolds obtained by the polymer replication method. Presence of macropores and interconnected porosity (a) and detailed view of the micropores (b).

2.2. Physical–chemical characterization

The microstructure of the hydroxyapatite powders and scaffolds was characterized using scanning electron microscopy (Hitachi S4700). The porous samples prior to observation were gold sputtered (Carringdon) and the powders coated with carbon ink.

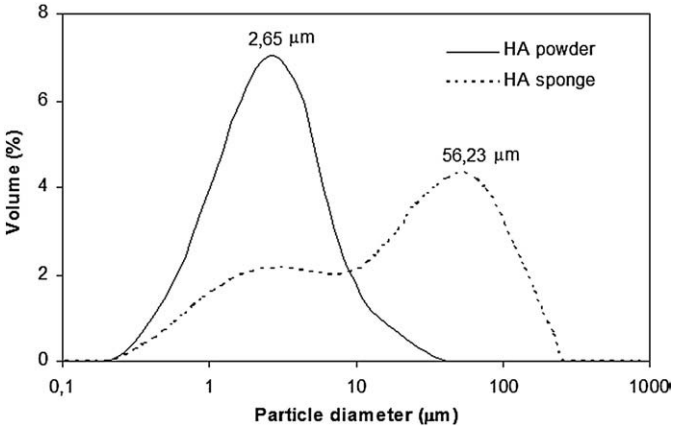

Fig. 4. Particle size distribution of the hydroxyapatite powder (starting material) and crushed sponges obtained by the replication method.

Please cite this article as: S. Teixeira, et al., Materials Science and Engineering C (2008), doi:10.1016/j.msec.2008.09.052

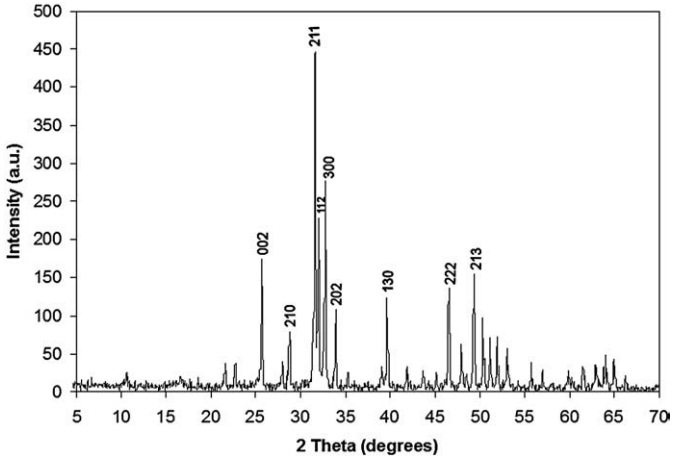

Fig. 5. X-ray diffraction pattern of the porous hydroxyapatite scaffolds obtained by the replication method.

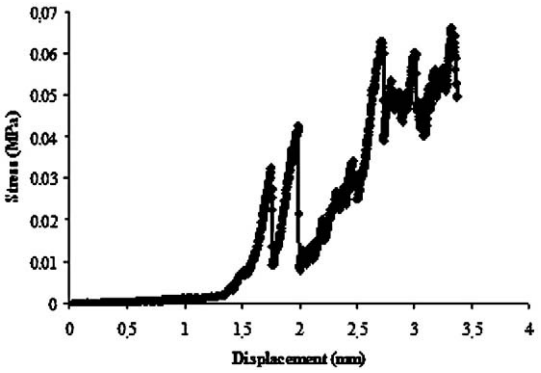

Fig. 7. Compressive stress/displacement curve of the porous hydroxyapatite scaffolds.

Particle size distribution was measured by Laser scattering (Mod. Mastersize by Malvern). The specific surface area was measured by the chromatographic method (mod. Monosorb from Quantachrome Inc.) using BET model.

The phases of the hydroxyapatite scaffolds were determined by X-ray diffraction using a Siemens diffractometer (D 5000 model) with CuKα radiation over the 2θ range of 5°–70° with a step size of 0.05°. In order to analyse the scaffolds, these were reduced to powder and spread over the analytical cylindrical sample holder. The mechanical compression testing of the hydroxyapatite scaffolds was performed using a Microtest equipment (Model 1114) using a 20 N load cell and a compression rate of 1 mm/min. FT-IR spectra were obtained using a Perkin Elmer 2000 System spectrometer with 100 scans per sample. Hydroxyapatite scaffolds were reduced to powder and analysed in the form of KBr pellets, using 1 mg of sample mixed with 300 mg of dry KBr. The mixture was homogenized in a Agata mortar. Pellets were obtained by compression in a 15 mm diameter die, under vacuum at 500 MPa of approximately 301 mg of the mixture per sample.

3. Results and discussion

The morphology of the hydroxyapatite powders used to produce the porous scaffold is shown in Figs. 1 and 2.

The hydroxyapatite powders used to produce the macroporous scaffolds possess an elongated shape and organize themselves as aggregates (Figs. 1 and 2).

The particles present an average diameter of ~50–100 nm (Fig. 1). In addition, dense powder aggregates with sizes of ~3 μm were observed (Fig. 2).

Using the polymer replication method, it was possible to produce highly porous hydroxyapatite scaffolds [11–13,25] as it may be seen in Fig. 3.

With SEM observations (Fig. 3), pore diameters ranging from 100 μm to 400 μm were observed. On the other hand, micropores from 1 μm to 10 μm were also visualised in the pores walls and struts. Taking into account the considerable presence of microporosity, it should be interconnected (as it is usual for values of microporosity above 10% in ceramics).

Particle size distribution of the crushed hydroxyapatite powders and scaffolds is shown in Fig. 4. The hydroxyapatite powder presents a mono-modal distribution with an average particle size of 2.65 μm, whereas the crushed hydroxyapatite scaffolds present a bimodal distribution with two maxima at ~2 and ~56 μm. The hydroxyapatite powders specific surface area is larger than that of the hydroxyapatite porous scaffolds, presenting values of 1.87 m^2/g and 0.80 m^2/g respectively.

Fig. 5 shows the X-ray diffraction patterns of the hydroxyapatite scaffolds. No new phase (after sintering) is formed and all peaks correspond solely to hydroxyapatite phase.

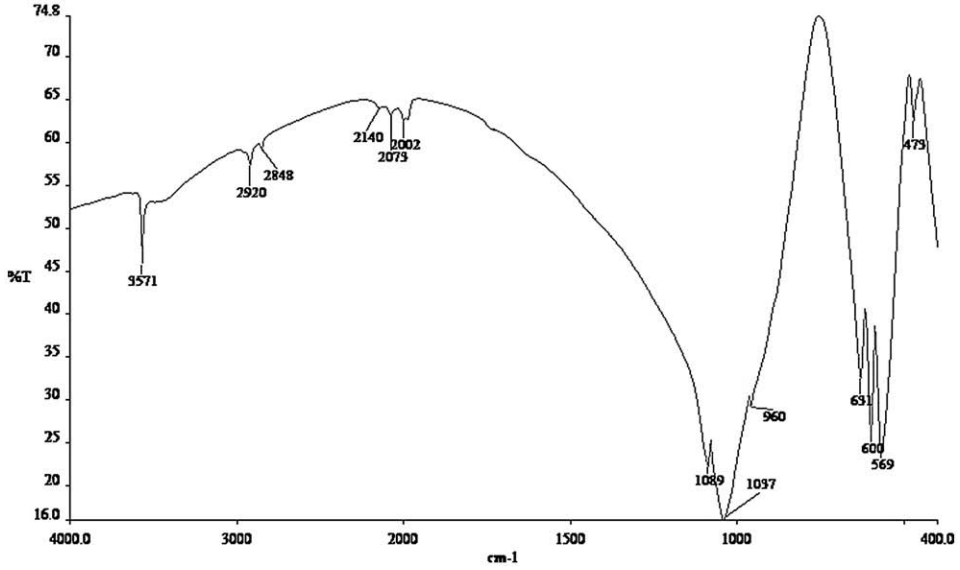

Fig. 6. Fourier transform infrared (FTIR) spectrum of the sintered hydroxyapatite sponge.

Please cite this article as: S. Teixeira, et al., Materials Science and Engineering C (2008), doi:10.1016/j.msec.2008.09.052

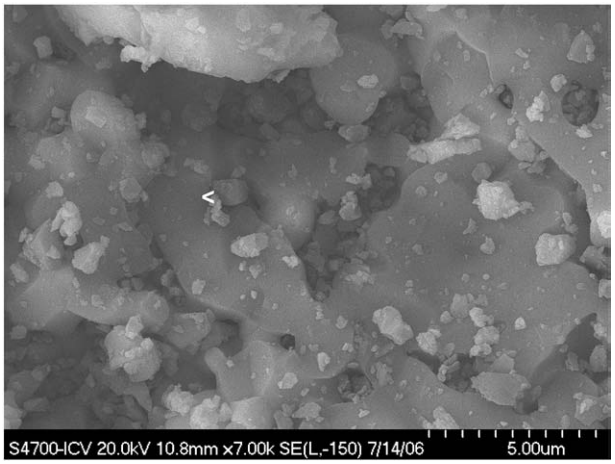

Fig. 8. Detailed SEM view of the porous hydroxyapatite scaffold fractured surface.

The FTIR spectrum of the sintered HA was obtained, presenting the characteristic peaks (Fig. 6).

There is a clear OH^- peak at 3571 cm^{-1}, followed by some broad peaks between 2920 and 2002 cm^{-1} that may correspond to HPO_4^{2-} groups as previously reported in the literature [26].

Phosphate υ_3 bands were identified by two peaks at 1089 and 1037 cm^{-1}, whereas the υ_1 band is present at 960 cm^{-1}.

Furthermore, the phosphate υ_2 band was also observed at 473 cm^{-1} being followed by phosphate υ_4 bands at peaks 602 and 504 cm^{-1}, respectively.

The samples were evaluated under compressive mechanical testing, with a maximum compressive stress value of 0.07 ± 0.03 N/mm^2. These values are in accordance with the literature [18].

A typical compressive stress/displacement curve of the porous samples may be seen in Fig. 7. The curve shows an early abrupt descent, with stress values increasing until a maximum was reached. However, this maximum value cannot be considered as the maximum compressive stress of sample, since it corresponds to sample densification after it had collapsed and free powders or small aggregates were being jointly compressed. It was visible as the assay progressed, that the sample started to aggregate quickly and therefore, increasing its resistance to the compressive force applied.

The pores started to be crushed and eventually the sample densification occurred and due to this phenomenon, some of the tested samples did not break.

On the other hand, higher compression resistance values may eventually be achieved if a more refined hydroxyapatite starting powder is employed. Moreover, mixing bioactive glass onto the initial ceramic slurry can also contribute for a more resistant scaffold [27]. Other reports show that the mechanical properties of these scaffolds prepared by this method can be increased with the addition of specific polymers, such as PLC [18]. One of the drawbacks of the polymer replication technique is the final thickness of the pore struts. Therefore, the addition of such elements (bioglasses or polymers) could lead to an increase in pore struts and in this manner, when solicited, the micropores would be able to withstand higher loads due to the coating migration to the inner pores [18,28].

The fracture point of the evaluated samples was localised at their centres with fracture cracks propagating towards their periphery. SEM observations showed that the scaffolds collapsed due to the reduced pore struts thickness.

As a result, those inner fracture surfaces were chosen to be assessed by SEM (Fig. 8).

The fracture surface is characterized by clear breakage (black arrows) showing a smooth fractured micropore surface with ceramic debris from the macropores.

4. Conclusions

In this work, it is shown that it was possible to produce porous scaffolds using a porous polymer sponge as a template.

The hydroxyapatite powders used as starting materials were characterized by presenting elongated shape and by their assembly into aggregates.

The hydroxyapatite starting powders presented a mono-modal distribution with an average particle size of 2.65 μm whereas the crushed hydroxyapatite scaffolds presents a bimodal distribution with particle size in the range of 2.65 μm and 56.23 μm. This fact can be explained by the likely formation of hard aggregates during sintering. This seems to be confirmed by the decrease of specific surface area when compared to that of the powders.

By SEM it was possible to observe that the porous hydroxyapatite scaffolds possess micropores and macropores that appear interconnected along the structure from the periphery until the centre, indicating that these are homogenous porous networks (Fig. 3).

The scaffolds are constituted by crystalline hydroxyapatite and no additional phase was formed during the polymer replication process as assessed by XRD and FTIR.

The compressive strength and SEM assays have indicated that the sponges fracture is initiated at their inner core and scaffolds collapsed due the reduced pore strut thickness.

The data obtained in this study show that the produced porous structures appear to have good conditions to be used as scaffolds for tissue engineering or even as a vehicle for the delivery of biological molecules. In vitro studies were already successfully carried out demonstrating the biocompatibility of the scaffolds in the presence of osteoblastic cells [13].

Currently, studies are being performed in order to incorporate collagen type I in these porous constructs, to improve their potential as bone mimicking scaffolds.

References

[1] A.C. Jones, B. Milthorpe, H. Averdunk, A. Limaye, T.J. Senden, A. Sakellariou, et al., Biomaterials 25 (20) (Sep 2004) 4947.
[2] V. Karageorgiou, D. Kaplan, Biomaterials 26 (27) (Sep 2005) 5474.
[3] P. Sepulveda, F.S. Ortega, M.D.M. Innocentini, V.C. Pandolfelli, Journal of the American Ceramic Society 83 (12) (Dec 2000) 3021.
[4] J.R. Woodard, A.J. Hilldore, S.K. Lan, C.J. Park, A.W. Morgan, J.A. Eurell, et al., Biomaterials 28 (1) (Jan 2007) 45.
[5] L.D. Harris, B.S. Kim, D.J. Mooney, Journal of Biomedical Materials Research 42 (3) (Dec 5 1998) 396.
[6] L.A. Cyster, D.M. Grant, S.M. Howdle, F.R. Rose, D.J. Irvine, D. Freeman, et al., Biomaterials 26 (7) (Mar 2005) 697.
[7] Q. Fu, M.N. Rahaman, B.S. Bal, W. Huang, D.E. Day, Journal of Biomedical Materials Research A 82 (1) (Jul 2007) 222.
[8] B.S. Chang, C.K. Lee, K.S. Hong, H.J. Youn, H.S. Ryu, S.S. Chung, et al., Biomaterials 21 (12) (Jun 2000) 1291.
[9] T.M. Chu, D.G. Orton, S.J. Hollister, S.E. Feinberg, J.W. Halloran, Biomaterials 23 (5) (Mar 2002) 1283.
[10] Q. Fu, M.N. Rahaman, F. Dogan, B.S. Bal, Journal of Biomedical Materials Research B, Applied Biomaterials (Dec 20 2007).
[11] A.C. Queiroz, S. Teixeira, J.D. Santos, F.J. Monteiro, Advanced Materials Forum Ii, vol. 455–456, 2004, p. 358.
[12] A.C. Queiroz, S. Teixeira, J.D. Santos, F.J. Monteiro, Bioceramics 254–2 (2004) 997 (16).
[13] S. Teixeira, M.P. Ferraz, F.J. Monteiro, Journal of Materials Science-Materials in Medicine 19 (2) (Feb 2008) 855.
[14] K. de Groot, Biomaterials 1 (1) (Jan 1980) 47.
[15] U. Heise, J.F. Osborn, F. Duwe, International Orthopaedics 14 (3) (1990) 329.
[16] Y. Kuboki, H. Takita, D. Kobayashi, E. Tsuruga, M. Inoue, M. Murata, et al., Journal of Biomedical Materials Research 39 (2) (Feb 1998) 190.
[17] H.R. Ramay, M. Zhang, Biomaterials 24 (19) (Aug 2003) 3293.
[18] H.W. Kim, J.C. Knowles, H.E. Kim, Journal of Materials Science 16 (3) (Mar 2005) 189.
[19] T. Iwano, H. Kurosawa, K. Murase, H. Takeuchi, Y. Ohkubo, Clinical Orthopaedics and Related Research 268 (Jul 1991) 243.
[20] Y. Tieliewuhan, I. Hirata, A. Sasaki, H. Minagi, M. Okazaki, Dental Materials Journal 23 (3) (Sep 2004) 258.
[21] S. Yunoki, T. Ikoma, A. Tsuchiya, A. Monkawa, K. Ohta, S. Sotome, et al., Journal of Biomedical Materials Research B, Applied Biomaterials 80 (1) (Jan 2007) 166.
[22] Q.Q. Zhang, L. Ren, C. Wang, L.R. Liu, X.J. Wen, Y.H. Liu, et al., Artificial Cells, Blood Substitutes, and Immobilization Biotechnology 24 (6) (Nov 1996) 693.

Please cite this article as: S. Teixeira, et al., Materials Science and Engineering C (2008), doi:10.1016/j.msec.2008.09.052

[23] S.M. Zhang, F.Z. Cui, S.S. Liao, Y. Zhu, L. Han, Journal of Materials Science 14 (7) (Jul 2003) 641.
[24] S. Yunoki, T. Ikoma, A. Monkawa, E. Marukawa, S. Sotome, K. Shinomiya, et al., Journal of Biomaterials Science 18 (4) (2007) 393.
[25] S. Teixeira, S. Oliveira, M.P. Ferraz, F.J. Monteiro, Key Engineering Materials 361–363 (II) (2008) 947.
[26] I.R. Gibson, S.M. Best, W. Bonfield, Journal of Biomedical Materials Research 44 (4) (Mar 15 1999) 422.
[27] M. Kamitakahara, C. Ohtsuki, Y. Kozaka, S. Ogata, M. Tanihara, T. Miyazaki, Journal of the Ceramic Society of Japan 114 (1325) (Jan 2006) 82.
[28] H.W. Kim, Y. Deng, P. Miranda, A. Pajares, D.K. Kim, H.E. Kim, et al., Effect of Flaw State on the Strength of Brittle Coatings on Soft Substrates, 2001, p. 2377.

Please cite this article as: S. Teixeira, et al., Materials Science and Engineering C (2008), doi:10.1016/j.msec.2008.09.052